Acid−Base Chemical Mechanism of Homocitrate Synthase from *Saccharomyces cerevisiae*†

Jinghua Qian, Ann H. West, and Paul F. Cook*

Department of Chemistry and Biochemistry, University of Oklahoma, 620 Parrington Oval, Norman, Oklahoma 73019

Received May 4, 2006; Revised Manuscript Received August 8, 2006

ABSTRACT: Homocitrate synthase (acetyl-coenzyme A:2-ketoglutarate C-transferase; E.C. 2.3.3.14) catalyzes the condensation of AcCoA and α-ketoglutarate to give homocitrate and CoA. The enzyme was found to be a Zn-containing metalloenzyme using inductively coupled plasma mass spectrometry. Dead-end analogues of α-ketoglutarate were used to obtain information on the topography of the α-ketoglutarate binding site. The α-carboxylate and α-oxo groups of α-ketoglutarate are required for optimum binding to coordinate to the active site Zn. Optimum positioning of the α-carboxylate, α-oxo, and γ-carboxylate of α-ketoglutarate is likely mimicked by the location in space of the 2-carboxylate, pyridine nitrogen, and 4 carboxylate of pyridine 2,4-dicarboxylate. The pH dependence of the kinetic parameters was determined to obtain information on the chemical mechanism of homocitrate synthase. The *V* profile is bell shaped with slopes of 1 and −1, giving pK_a values of 6.7 and 8.0, while V/K_{AcCoA} exhibits a slope of 2 on the acidic side with an average pK_a value of 6.6 and a slope of −2 on basic side of the profile with an average pK_a value of 8.2. The $V/K_{\alpha-Kg}$ pH−rate profile exhibits a single pK_a of 6.9 on the acidic side and two on the basic side with an average value of 7.8. The pH dependence of the K_i for glyoxylate, a competitive inhibitor vs α-ketoglutarate, gives a pK_a of 7.1 for a group, required to be protonated for optimum binding. Data suggest a chemical mechanism for the enzyme in which α-ketoglutarate first binds to the active site Zn via its α-carboxylate and α-oxo groups, followed by acetyl-CoA. A general base then accepts a proton from the methyl of acetyl-CoA, and a general acid protonates the carbonyl of α-ketoglutarate in the formation of homocitryl-CoA. The general acid then acts as a base in deprotonating Zn-OH_2 in the hydrolysis of homocitryl-CoA to give homocitrate and CoA. A solvent deuterium kinetic isotope effect of 1 is measured for homocitrate synthase, while a small pH-independent primary kinetic deuterium isotope effect (∼1.3) is observed using deuterioacetyl-CoA. Data suggest rate-limiting condensation to form the alkoxide of homocitryl-CoA, followed by hydrolysis to give products.

Homocitrate synthase (HCS)[1] (acetyl-coenzyme A:2-ketoglutarate C-transferase; E.C. 2.3.3.14) catalyzes the first and regulated step in the α-aminoadipate pathway for lysine synthesis (*1*, *2*). Lysine is the only essential amino acid that has two distinct biosynthetic pathways: the diaminopimelate pathway in plants, bacteria, and lower fungi and the α-aminoadipate pathway in Euglenoids and higher fungi which include human pathogens such as *Candida albicans*, *Cryptococcus neoformis*, and *Aspergillus fumigatus* and plant pathogens like *Magnaporthe grisea* (*3*, *4*). Because of the uniqueness of the pathway, it is a potential target for antifungal drugs.

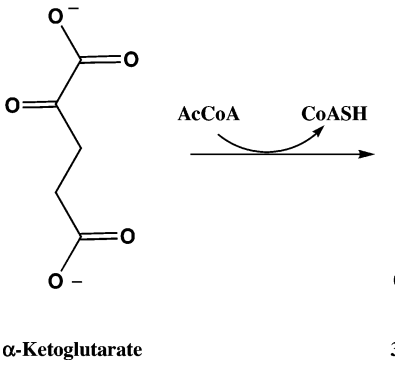

(1)

The enzyme catalyzes the condensation of AcCoA and α-Kg to form homocitrate and CoA (eq 1). The histidine-tagged homocitrate synthase from *Saccharomyces cerevisiae* has been overexpressed in *Escherichia coli* and purified to about 98% using a Ni-NTA resin (*8*). As isolated, HCS is not stable (*5*−*7*) but can be stabilized using additives including guanidine hydrochloride, α-cyclodextrin,

† This work was supported by the Grayce B. Kerr Endowment to the University of Oklahoma (to P.F.C.), by a grant (GM 071417) from the National Institutes of Health (to P.F.C. and A.H.W.), and by a grant-in-aid from the Office of the Research and Administration at the University of Oklahoma (to P.F.C. and A.H.W.).

* Corresponding author. E-mail: pcook@chemdept.chem.ou.edu. Tel: 405-325-4581. Fax: 405-325-7182.

[1] Abbreviations: HCS, homocitrate synthase; Hc, homocitrate; IPMS, isopropylmalate synthase; CoA, coenzyme A; AcCoA, acetyl-CoA; α-Kg, α-ketoglutarate; DCPIP, 2,6-dichlorophenolindophenol; EDTA, ethylenediaminetetraacetic acid; ICP-MS, inductively coupled plasma mass spectrometry; Mes, 2-morpholinoethanesulfonic acid; Taps, *N*-[tris(hydroxymethyl)methyl]-3-aminopropanesulfonic acid; Hepes, 4-(2-hydroxyethyl)-1-piperazineethanesulfonic acid.

10.1021/bi060889h CCC: $33.50
Published on Web 09/09/2006

and ammonium sulfate so that it can be stored for at least 2 months at 4 °C (*8*). The synthase catalyzes a predominantly ordered Bi-Bi reaction with α-ketoglutarate binding to the enzyme first, followed by acetyl-CoA. After hydrolysis of the homocitryl-CoA intermediate, CoA is released prior to homocitrate (*9*).

To date, nothing is known of the chemical mechanism of HCS. In this paper, the pH dependence of the kinetic parameters, isotope effects, and dissociation constants for competitive inhibitors are used to probe the chemical mechanism of HCS. A general acid−base chemical mechanism is proposed.

MATERIALS AND METHODS

Chemicals. α-Ketoglutarate, AcCoA, CoA, DCPIP, oxaloacetate, α-ketomalonate, α-ketobutyrate, pyruvate, adipate, glutarate, malonate, glyoxylate, pyridine 2,6-dicarboxylate, pyridine 2,4-dicarboxylate, pyridine 2,3-dicarboxylate, pyridine 2,5-dicarboxylate, pyridine 2-carboxylate, pyridine 4-carboxylate, EDTA, 1,10-phenanthroline, and imidazole were obtained from Sigma. *N*-Oxalylglycine was obtained from Frontier Scientific. Glycerol, succinate, oxalate, KCl, $CaCl_2$, $MgCl_2$, $MnCl_2$, $ZnCl_2$, and guanidine hydrochloride were from Fisher Scientific, while $(NH_4)_2SO_4$ was obtained from Fluka. Taps, Hepes, and Mes were from Amresco. Perdeuterioacetic anhydride (98 atom % D) and D_2O (99 atom % D) were purchased from Cambridge Isotope Laboratories, Inc. Succinyl phosphonate was synthesized according to the method of Gibson et al. (*10*).

The deuterioacetyl-CoA was prepared from CoA and perdeuterioacetic anhydride according to the method of Simon and Shemin (*11*). The deuterioacetyl-CoA exhibited a single peak with baseline separation from CoA when chromatographed isocratically on a C_{18} HPLC column with a solvent containing 220 mM potassium phosphate (pH 5.3) and 20% (v/v) CH_3OH (*12*). The ratio of absorbance at 260 to 233 nm reported for acetyl-CoA, deuterioacetyl-CoA, and CoA were 1.8, 1.84, and 3.65, respectively (*13*). The ratio obtained for the sample synthesized is 1.72, indicating no contaminating CoA. Deuterioacetate does not influence the activity of the enzyme. The concentrations of AcCoA and DCPIP stock solutions were adjusted spectrophotometrically, using the following extinction coefficients: AcCoA, $\epsilon_{260} = 16.4\ mM^{-1}\ cm^{-1}$; DCPIP, $\epsilon_{600} = 19.1\ mM^{-1}\ cm^{-1}$.

Cell growth, HCS expression, purification, and stabilization of the purified enzyme were the same as reported previously (*8*). Before each assay, 10% glycerol was added to completely dissolve the stabilizing agents in the stock enzyme solution.

Enzyme Assay. HCS activity was measured using the DCPIP assay developed previously (*8*), monitoring the decrease in absorbance at 600 nm as DCPIP is reduced. Reactions were carried out in quartz cuvettes with a path length of 1 cm in a final volume of 0.5 mL containing 50 mM Hepes, pH 7.5, 0.1 mM DCPIP, and variable concentrations of α-Kg and AcCoA. Assays were carried out at room temperature.

ICP-MS Analysis. Purified enzyme (0.673 mg/mL) was dialyzed against doubly distilled water overnight. The sample, in a polypropylene tube, was sent to Elemental Research Inc., Canada, for ICP-MS analysis. The doubly distilled water was also sent as a control in a separate analysis for Zn content.

pH Studies. The pH dependence of *V* and *V/K* for both substrates was obtained by varying one substrate with the other one maintained at a saturating concentration ($10K_m$). In order to obtain estimates of the K_m values for α-Kg and AcCoA as a function of pH, initial velocity patterns were obtained at pH 6.2 and 8.6 by measuring the initial velocity at different levels of α-Kg and different fixed levels of AcCoA. The pH was maintained using the following buffers at 200 mM concentration: Mes, 6.0−7.0; Hepes, 7.0−8.0; Taps, 8.0−9.0. The pH was recorded before and after initial velocity data were measured. The enzyme is stable when incubated for 10 min over the pH range 6−9.

pH profiles were then obtained by plotting log *V* or log(*V/K*) against pH, while the inhibition profile for glyoxalate was obtained by plotting $\log(1/K_i)$ against pH. Inhibition constants were obtained for inhibitors competitive with α-Kg at a fixed concentration of AcCoA ($10K_m$) and different fixed levels of inhibitor including zero. (The inhibition constant for glyoxalate was also measured in D_2O at pD 9.) When oxalylglycine was used as an inhibitor, data were obtained with AcCoA equal to 30 K_m and at $3K_m$. Lower concentrations of AcCoA gave very low initial rates.

Isotope Effects. Primary deuterium isotope effects were measured by direct comparison of initial velocities, where deuterioacetyl-CoA was used as the deuterated substrate and α-Kg was fixed ($5K_m$). For solvent deuterium isotope effects, the same reagents used in H_2O were prepared in D_2O by dissolving the reagent in a small amount of D_2O, lyophilizing overnight to remove H_2O, and redissolving the residue in D_2O. Data were obtained with AcCoA as the variable substrate at a fixed concentration of α-Kg ($5K_m$). The isotope effects were obtained by direct comparison of initial rates in H_2O and D_2O over the pH(D) range 6.8−8.0, around the pH-independent region of the *V* and *V/K* pH−rate profile.

Deuterium Washout. A reaction mixture was prepared containing 1 mM deuteriomethylacetyl-CoA and 50 mM α-Kg. Enzyme was added to initiate the reaction, which was allowed to proceed to 50% completion. The reaction was terminated by freezing, enzyme was separated, and ^1H NMR was used to determine whether the methyl group contained protons. No protons were observed. Controls included acetyl-CoA, which gave a signal at 1.4 ppm, and deuteriomethylacetyl-CoA, which gave no signal. All spectra were obtained on a Varian Mercury VX-300 MHz NMR spectrometer.

Data Analysis. Data were fitted to appropriate equations as discussed below, using the Marquardt−Levenberg algorithm supplied with the EnzFitter program from BIOSOFT, Cambridge, U.K. Kinetic parameters and their corresponding standard errors were estimated using a simple weighing method. Data for individual saturation curves, initial velocity patterns obtained at pH 6.2 and 8.6, and competitive inhibition patterns were fitted using eqs 2−4. Data for *V* and *V/K* deuterium isotope effects were fitted using eq 5.

$$v = \frac{VA}{K_a + A} \quad (2)$$

$$v = \frac{VAB}{K_{ia}K_b + K_aB + K_bA + AB} \quad (3)$$

$$v = \frac{VA}{K_a(1 + I/K_{is}) + A} \quad (4)$$

$$v = \frac{VA}{K_a(1 + F_iE_{V/K}) + A(1 + F_iE_V)} \quad (5)$$

In eqs 2−5, v is the initial velocity, V is the maximum velocity, A, B, and I are reactant and inhibitor concentrations, K_a and K_b are Michaelis constants for A and B, K_{ia} and K_{is} are inhibition constants for A and slope, respectively, F_i is the fraction of D_2O in the solvent or deuterium label in the substrate, and $E_{V/K}$ and E_V are the isotope effects −1 on V/K and V, respectively.

Data for pH−rate profiles that decreased with a slope of 1 at low pH and a slope of −1 at high pH were fitted by using eq 6. Data for pH−rate profiles with a slope of 1 at low pH and a slope of −2 at high pH were fitted by using eq 7, while data for pH−rate profiles with a slope of 2 at low pH and a slope of −2 at high pH were fitted by using eq 8. Data for pK_i profiles were fitted by using eq 9.

$$\log y = \log\left[C/\left(1 + \frac{H}{K_1} + \frac{K_2}{H}\right)\right] \quad (6)$$

$$\log y = \log\left[C/\left(1 + \frac{H}{K_1} + \frac{K_2}{H} + \frac{K_2K_3}{H^2}\right)\right] \quad (7)$$

$$\log y = \log\left[C/\left(1 + \frac{H}{K_1} + \frac{H^2}{K_1K_2} + \frac{K_3}{H} + \frac{K_3K_4}{H^2}\right)\right] \quad (8)$$

$$\log y = \log\left[\frac{Y_L + Y_H\left(\frac{K_1}{H}\right)}{1 + \frac{K_1}{H}}\right] \quad (9)$$

In eqs 6−9, K_1, K_2, K_3, and K_4 represent acid dissociation constants for enzyme or reactant functional groups, y is the value of the parameter observed as a function of pH, C is the pH-independent value of y, H is the hydrogen ion concentration, and Y_L and Y_H are constant values of $1/K_i$ at low and high pH, respectively.

RESULTS

ICP-MS Data. Homocitrate synthase is inactivated in the presence 1,10-phenanthroline (*2*), dipicolinic acid, and EDTA, which are metal-chelating reagents. Once the enzyme has been inactivated by EDTA, it can be reactivated by the addition of 5 mM Zn^{2+} or Mn^{2+}. To test whether the enzyme has a tightly bound metal ion, a sample was dialyzed overnight against doubly distilled water and sent to Elemental Research Inc., Canada, for a full scan of metal ions by ICP-MS. Results indicated that the enzyme solution contained Na^+, K^+, Zn^{2+}, Ca^{2+}, and Si^{2+}. Among the metal ions found only Zn^{2+} can reactivate the enzyme. It is difficult to estimate the stoichiometry of Zn bound to HCS, because the enzyme precipitated when stabilizing agents were removed as the sample was prepared for analysis. However, the stoichiometry of Zn bound per HCS subunit is about 1.

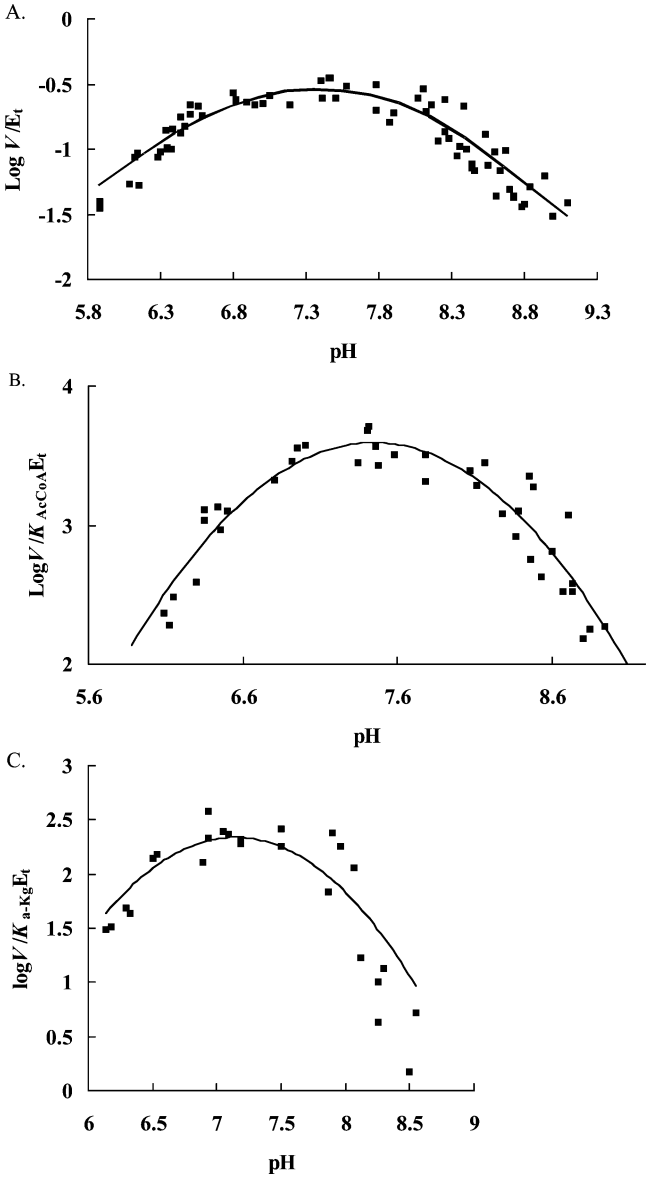

FIGURE 1: pH dependence of kinetic parameters for the HCS reaction from *S. cerevisiae*. Data were obtained at room temperature for V (A), V/K_{AcCoA} (B), and $V/K_{\alpha-Kg}$ (C). The points shown are the experimentally determined values, while the curves are theoretical, based on fits of the data using eq 6 for V, eq 8 for V/K_{AcCoA}, and eq 7 for $V/K_{\alpha-Kg}$.

pH Dependence of Kinetic Parameters. The pH dependence of the kinetic parameters for HCS was determined, and the results are shown in Figure 1. The maximum velocity decreases at high and low pH, giving pK values of 6.7 and 8.0. The V/K for AcCoA decreases at low pH, with a slope of 2 giving an average pK of 6.6 and with a slope of −2 at high pH giving an average pK of 8.2. The V/K for α-Kg decreases at low pH, with a slope of 1 giving a pK of 6.9 and with a slope of −2 at high pH giving an average pK value of 7.8. pK_a values are summarized in Table 1. The pH-independent values of V/E_t, $V/K_{AcCoA}E_t$, and $V/K_{\alpha-Kg}E_t$ are 0.33 ± 0.03 s^{-1}, (5.6 ± 0.4) × 10^3 M^{-1} s^-, and 610 ± 40 M^{-1} s^{-1}.

Table 1: pH Dependence of Kinetic Parameters for HCS from *S. cerevisiae*

parameter	acidic side pK ± SE	basic side pK ± SE
V	6.7 ± 0.1 (1)[a]	8.0 ± 0.1 (1)
V/K_{AcCoA}	6.6 ± 0.1[b] (2)	8.2 ± 0.1[b] (2)
$V/K_{\alpha-Kg}$	6.9 ± 0.5 (1)	7.8 ± 1.5[b] (2)
$pK_{i\ glyoxalate}$		7.1 ± 1.3 (1)
		8.0 ± 0.2[c] (1)

[a] Values in parentheses indicate the number of groups associated with the pK_a. [b] Average value. [c] pK_a in the E·glyoxalate complex.

Table 2: K_i Values of α-Kg Analogues[a]

inhibitor	K_i (mM)
α-Kg	26[b]
oxalylglycine	7.7 ± 1.5
oxaloacetate	4[b]
glyoxylate	0.4 ± 0.2
oxalate	1 ± 0.2
α-ketomalonate	10 ± 2
glutarate	26 ± 1
pyridine 2-dicarboxylate	0.43 ± 0.04
pyridine 2,6-dicarboylate	0.7 ± 0.1
pyridine 2,4-dicarboylate	0.6 ± 0.1
pyridine 2,3-dicarboxylate	3.0 ± 0.7
pyridine 2,5-dicarboylate	14 ± 1
succinyl phosphonate	46 ± 9

[a] Experiments were carried out at room temperature, pH 7.2. The concentration of α-Kg was varied around its K_m value while that of AcCoA was fixed at 30 μM (10K_m) (for oxalylglycine AcCoA was 0.1 mM). All of the compounds listed are competitive inhibitors of HCS versus α-Kg. [b] K_d value from ref *9*.

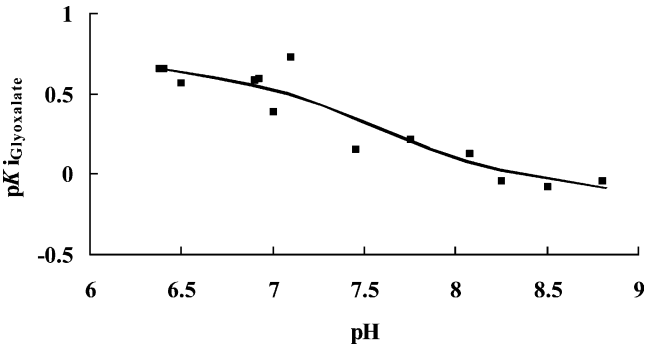

FIGURE 2: pH dependence of the reciprocal of the inhibition constant for glyoxalate. The points shown are the experimentally determined values, while the curve is theoretical, based on the fit of the data using eq 9.

Inhibition Data. A number of analogues of α-Kg were tested to see whether they are substrates or inhibitors of HCS at pH 7.2. Results are shown in Table 2. In addition to the compounds listed in Table 2, α-ketobutyrate, pyruvate, adipate, succinate, malonate, and pyridine 4-carboxylate gave no observed inhibition at a concentration of 50 mM.

The pH dependence of the K_i for oxalylglycine, oxalate, and glyoxylate, inhibitors competitive against α-ketoglutarate, was determined in order to obtain an estimate of the intrinsic pK value(s) of group(s) required for optimum binding of the keto acid. The $pK_{i\ glyoxalate}$ profile is shown in Figure 2. The pK_i decreases from a constant value at pH 6 and below to another constant value above pH 8. A pK of about 7.1 is estimated for free enzyme, and this pK is perturbed to about 8 in the E·glyoxalate complex (Table 1).

		32	212 214
S. cerevisiae	Homocitrate synthase	LRE**G**E	EC**H**F**H** ND
T. thermophilus	Homocitrate synthase	LRE**G**E	EF **H**G**H** ND
C. pasteurianum	Homocitrate synthase	LRD**G**E	EI **H**V**H** ND
M. maripaludis	Citramalate synthase	LRD**G**E	SI **H**C**H** ND
M. jannaschii	Citramalate synthase	LRD**G**E	SV**H**C**H** ND
T. elongatus	Isopropylmalate synthase	LRD**G**E	SV**H**G**H** ND
E. coli	Isopropylmalate synthase	LRD**G**E	SV**H**T**H** DD
P. abyssi	Isopropylmalate synthase	LRD**G**S	GI **H**A**H** ND
S. cerevisiae	Isopropylmalate synthase	LRD**G**N	ST **H**C**H** ND
M. tuberculosis	Isopropylmalate synthase	LRD**G**N	SL **H**P**H** ND
		*	* *

FIGURE 3: Sequence alignment of the protein residues coordinated with the Zn ion. Homocitrate synthase, isopropylmalate synthase, and citramalate synthase all share significant sequence similarity.

The pH-independent dissociation constant for glyoxylate is 0.19 ± 0.02 mM for E·glyoxalate and increases to 1.4 ± 0.3 mM in EH·glyoxalate. Given an equilibrium constant of 260 in favor of the hydrated aldehyde (*28*), it was anticipated that the hydrated form of glyoxalate, the *gem*-diol, bound to enzyme and not the aldehyde form. An inverse solvent deuterium isotope effect of about 0.84 is obtained on the equilibrium constant for hydration of the aldehyde (*29*). The $K_{i\ glyoxalate}$ measured at pD 9 is 0.5 ± 0.1 mM, a factor of 2 lower than that measured in H_2O. Data suggest that the hydrated or diol form of glyoxalate binds to enzyme. The $pK_{i\ oxalate}$ vs pH profile is qualitatively identical to that obtained for glyoxalate (data not shown). pH-independent dissociation constants of 0.6 ± 0.1 and 11 ± 2 mM are estimated at low and high pH, respectively. The K_i for oxalylglycine increases by only about a factor of 3 as the pH is increased from 6.2 to 8 (data not shown). The K_i estimated at pH 7.2 is 7.7 ± 1.5 mM with AcCoA equal to $30K_{AcCoA}$ (Table 2). With AcCoA decreased to $3K_{AcCoA}$, the K_i of oxalylglycine decreased from 8 to 3 mM at pH 7.2.

Isotope Effects. A solvent kinetic deuterium isotope effect of 1 was observed for the HCS reaction. A small finite primary kinetic deuterium isotope effect is obtained when deuteriomethyl-AcCoA is used with $^{D}V = 1.36 \pm 0.24$ and $^{D}(V/K_{AcCoA}) = 1.54 \pm 0.18$ at pH 6.3, $^{D}V = 1.32 \pm 0.11$ and $^{D}(V/K_{AcCoA}) = 1.29 \pm 0.14$ at pH 7.2, and $^{D}V = 1.36 \pm 0.24$ and $^{D}(V/K_{AcCoA}) = 1.2 \pm 0.21$ at pH 8.5.

Deuterium Washout. No protons were detected by ^{1}H NMR after the reaction had proceeded to 50%. Data suggest that if deprotonation of the methyl group of AcCoA comes to equilibrium, then the protonated base does not exchange with bulk solvent.

DISCUSSION

HCS Is a Zn-Containing Metalloenzyme. On the basis of the ICP-MS analysis, HCS is likely a Zn-containing metalloenzyme, similar to the homologous IPMS from *S. cerevisiae* (*14*). Recently, the structure of IPMS, a homologue of HCS, was solved and shown to be a Zn-containing metalloenzyme (*15*). In the IPMS, three ligands to Zn^{2+}, Asp81, His285, and His287, are conserved in HCS (Glu32, His212, and His214) and citramalate synthase (Figure 3). In the structure of the IPMS complexed with α-ketoisovalerate, the α-carboxylate and α-keto of the substrate are also coordinated to the Zn^{2+}. It is likely that Zn^{2+} in HCS plays a role similar to that in IPMS, given the identity of ligands coordinated to the metal ion in both cases.

Vallee et al. (*16*−*18*) have suggested that a catalytic Zn is coordinated by three amino acid residues of the protein

with a binding preference of His ≫ Glu ≫ Asp = Cys. The spacing between the first two ligands is usually only one to three amino acids to provide a nucleus for zinc binding, while the spacing between the third ligand and the first two ligands is usually greater, which brings into alignment amino acid residues involved in catalysis and creates a substrate binding pocket. This latter situation is observed in HCS, IPMS, and citramalate synthase.

Interpretation of the Inhibition Data. Detailed information on the binding site of a metalloenzyme using α-Kg as a substrate has been obtained, for example, for prolyl 4-hydroxylase and γ-butyrobetaine hydroxylase (*19*−*21*). Two classes of inhibitor, aliphatic and aromatic, were chosen as probes of the α-Kg binding site of HCS. With the exception of the compounds that exhibit no inhibition at high concentrations, all other compounds are competitive inhibitors of HCS versus α-Kg. From these data, the topography of the α-Kg site has been obtained with respect to (1) the C5 carboxylate, (2) the C1−C2 unit of α-Kg, and (3) the spatial relationship and distance between C5 carboxylate and the C1−C2 unit. Inhibition constants are summarized in Table 2.

The requirement for the C5 carboxyl group is evident from the effects of omitting it. Inhibition is not observed for α-ketobutyrate and pyruvate even at concentrations as high as 50 mM.

The importance of the α-carboxylate and α-oxo groups which coordinate to the active site Zn ion is evident from the behavior of aliphatic and aromatic inhibitors. Succinate, malonate, and adipate, which lack the α-carbonyl, do not inhibit the enzyme, even at high concentrations. Oxaloacetate is a substrate with a K_d of 4 mM (*9*), while α-ketomalonate also inhibits the enzyme. In addition, pyridine 2,3-dicarboxylate, pyridine 2,4-dicarboxylate, pyridine 2,5-dicarboxylate, and pyridine 2-carboxylate are competitive inhibitors versus α-Kg. All likely coordinate the Zn ion via the ring nitrogen and the C2 carboxylate. If the position of the carboxylate is changed, e.g., pyridine 4-carboxylate, no inhibition is observed, even at high concentrations of the inhibitor. Data suggest that the α-carboxylate/α-oxo moieties of α-Kg are essential for optimal binding of the substrate.

For the pyridine carboxylate inhibitors, the pyridine 2-carboxylate configuration is optimal. The nitrogen atom in the pyridine ring acts as the oxygen atom of the carbonyl group to coordinate to the Zn ion. Addition of a second carboxylate at a different position on the pyridine ring can also be accommodated. In the three compounds with different spatial arrangement, pyridine 2,4-dicarboxylate, pyridine 2,3-dicarboxylate, and pyridine 2,5-dicarboxylate, the 2,4-dicarboxylate has the lowest K_i value, 0.59 mM at pH 7.2, while the K_i value of pyridine 2,5-dicarboxylate has increased to 14 mM. Thus, a carboxylate at the 2 and 4 positions provides the tightest binding. Since pyridine 2,6-dicarboxylate likely provides a terdentate coordination with the Zn ion, which is different from the bidentate coordination provided by the other analogues, it is not discussed here.

The distance between the C1−C2 unit and the C5 carboxylate is another important factor for the binding of the substrate. Oxaloacetate, which is a methylene group shorter than α-Kg, can still act as a substrate, though its K_m has increased to 25 mM (*9*) compared to 3 mM for α-Kg. Data may suggest synergism of binding in the case of α-Kg and AcCoA but not in the case of OAA and AcCoA. The kinetic mechanism of the HCS is ordered (*9*), and synergism is difficult to reconcile. In addition, the K_i value for oxalylglycine decreases to 3 mM at pH 7.2 when the concentration of AcCoA is decreased, inconsistent with synergism. The K_d for E·OAA is 6-fold lower than that of α-Kg, suggesting that there may be strain in accommodating the additional methylene in the longer substrate. However, the K_d for OAA is only a little over 2-fold lower than that estimated for oxalylglycine. The reason for the difference in K_i for α-Kg and OAA is at present unknown.

Pyridine 2,4-dicarboxylate has a lower dissociation constant than oxaloacetate and α-Kg (Table 2). The distance between the two carboxylates is 3.77 Å in the case of pyridine 2,4-dicarboxylate, similar to α-Kg in its extended conformation (3.83 Å). (Data were obtained from the Cambridge Structural Database.) It is thus likely that the planar nature of the pyridine optimally places the two negative charges in the case of the pyridine dicarboxylate, which is likely not true in the case of OAA or α-Kg. α-Ketomalonate, a three-carbon dicarboxylic acid, acts as a weaker inhibitor, indicating a likely difference in conformation with both of its carboxylates coordinated to Zn.

The C1−C2 unit of α-Kg appears to be the most important moiety for the binding of inhibitors and, by analogy, substrates. Glyoxylate, oxalate, and pyridine 2-carboxylate are the best inhibitors, although they do not have the C5 carboxylate group, while no inhibition is observed for adipate, succinate, and malonate, which do not have an integral C1−C2 unit. The inhibition constant of glyoxylate is lower than that of oxalate though both of them have the same carbon chain length. This is due to the additional negative charge on oxalate, which may be in close proximity to a negatively charged group in the vicinity of the Zn ion.

Interpretation of the pH Dependence of Kinetic Parameters. The pH dependence of log *V* versus pH is obtained at saturating concentrations of substrates, while log *V*/*K* versus pH is obtained at a limiting concentration of one of the reactants and saturating levels of all others. The *V* profile will thus reflect groups on the enzyme required for catalysis, while the *V*/*K* profile will reflect titratable groups on free enzyme ($V/K_{\alpha-Kg}$), E·α-Kg (V/K_{AcCoA}), and/or reactant important for binding and/or catalysis (*22*). In the case of an ordered mechanism, the *V*/*K* for the first substrate reflects the rate constant for binding reactant to enzyme and will thus reflect groups important for binding, which may also contribute to catalysis, for example, if a catalytic group hydrogen bonds the substrate.

The *V* pH−rate profile exhibits slopes of 1 and −1, indicating the requirement for one group protonated and another unprotonated for catalysis (Figure 1A). The group with a p*K* of 6.7, that must be unprotonated, likely functions as a general base to abstract a proton from the methyl group of acetyl-CoA. The group with a p*K* of about 8.0, that must be protonated, may be a general acid that hydrogen bonds to the carbonyl group of α-Kg and donates a proton to form the alcohol as the methyl of AcCoA attacks.

In the case of the V/K_{AcCoA} pH−rate profile (Figure 1B), slopes of 2 and −2 are observed, suggesting that two groups must be unprotonated and two groups must be protonated for binding and/or catalysis at limiting AcCoA. Since AcCoA is the last substrate bound to the enzyme, the protonation

Scheme 1: Proposed Chemical Mechanism for Homocitrate Synthase

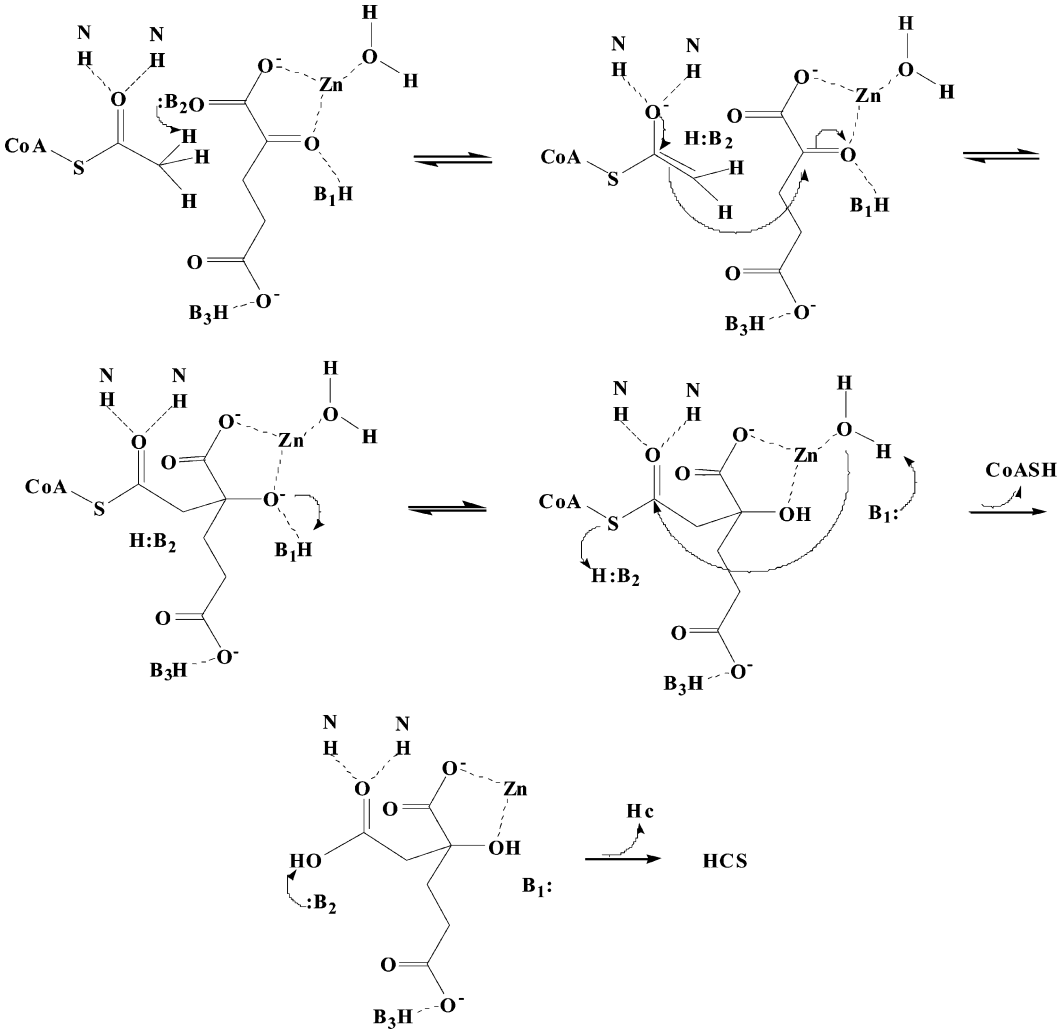

state of groups important for binding of AcCoA and/or catalysis in the E•α-Kg complex and free AcCoA will be observed. One of the groups that must be unprotonated and one that must be protonated are likely also observed in the *V* profile. The p*K* values obtained on the acid and base side of the profile agree within error with those observed in the *V* pH−rate profile (Table 1). The additional groups observed in the *V*/*K* profile that must be protonated and unprotonated are likely required for binding of AcCoA. The residues that must be unprotonated have an average p*K* value of 6.6, while the residues that must be protonated have an average p*K* value of 8.2. In the case of the CoA-dependent acyltransferases the binding of CoA is facilitated by a positively charged residue, Arg or Lys, positioned to interact with the 3′-phosphate of CoA or AcCoA (*23*). It is likely that the 3′-phosphate of acetyl-CoA must be unprotonated for optimum binding, while the group that must be protonated may, by analogy, be a Lys residue. The 3′-phosphate of AcCoA has a p*K* value of 6.4 (*24*), within error identical to the p*K* obtained from the V/K_{AcCoA} pH−rate profile. The p*K* value for the putative lysine residue is 8.2.

For the $V/K_{\alpha-Kg}$ pH−rate profile (Figure 1C), slopes of 1 and −2 are observed, suggesting that two residues must be protonated and one residue must be unprotonated for binding of α-Kg. The residues that must be protonated have an average p*K* of 7.8, and one of these likely serves as a hydrogen bond donor to the carbonyl of α-Kg and donates its proton in the condensation step; it is also observed in the *V* profile (p*K* = 8.0). The second of the groups with a p*K* of 7.8 is likely one that must be protonated to hydrogen bond to the γ-carboxylate of α-Kg. The function of the group with a p*K* value of 6.9 that must be unprotonated for binding is not known.

The K_m value of AcCoA obtained at optimum pH is around 50 μM, about 10-fold higher than that reported previously (2 μM) (*9*). The higher value results from the high concentration of potassium ion in the assay. Potassium is an inhibitor that competes with AcCoA (*25*, *26*). None of the other kinetic parameters are affected by the presence of K^+.

In order to determine whether true p*K* values are obtained in the pH−rate profile, glyoxylate, oxalate, and oxalylglycine were chosen as dead-end inhibitors of α-Kg to measure pK_i profiles. Over the pH range studied, all three are competitive inhibitors versus α-Kg. The pK_i decreases as the pH is increased above 7 to a constant value at high pH. A p*K* value of 7.1 is observed for a group in free enzyme that must be protonated for optimum binding of glyoxalate, while the p*K* increases to 8.0 when glyoxylate is bound. Although the quantitative changes in K_i differ between the three, the pH dependence of the K_i is similar for all three inhibitors. The p*K* of 8−8.2 for the EHI complex agrees with the value observed in the *V* pH−rate profile, under conditions where

α-Kg is bound. Thus, the carbonyl of the substrate interacts with the Zn ion and an enzyme residue. Deprotonation of the residue results in a 7-fold decrease in affinity for glyoxylate and, by analogy, α-Kg.

Interpretation of Isotope Effects. A solvent kinetic deuterium isotope effect of 1 was observed for the HCS reaction. This suggests that protons are not in flight in the rate-determining transition state. A small pH-independent primary kinetic isotope effect of about 1.3 is observed using deuteriomethylacetyl-CoA. An equilibrium isotope effect of about 1.13/D would be expected on the enolization of AcCoA as carbon goes from sp^3 to sp^2 (*27*), giving a value of 1.28, within error equal to the observed value of 1.3. Thus, it is likely that the enolization of AcCoA comes to equilibrium prior to the condensation reaction. Since no solvent kinetic isotope effect is observed, it is unlikely that the hydrolysis of homocitryl-CoA is slow and thus the condensation reaction likely limits overall. However, the lack of a solvent isotope effect suggests the product of the condensation reaction may be a Zn-bound alkoxide, which then receives a proton from the general acid with a p*K* of 8.

Proposed Chemical Mechanism. A chemical mechanism can thus be proposed on the basis of the findings discussed above and is shown in Scheme 1. α-Kg binds to the enzyme with its α-carboxylate and α-oxo groups coordinated to the active site Zn^{2+}. At this point the Zn is coordinated to two imidazoles, a glutamate, the α-carboxylate and α-oxo of α-Kg, and a water molecule (based on analogy to IPMS). A general acid, B_1, donates a hydrogen bond to the carbonyl of α-Kg, while the C5 carboxylate interacts with a protonated residue on the enzyme, B_3H. AcCoA then binds with its thioester oxygen either interacting with a conserved arginine (based on analogy to IPMS) or in an anion hole and its methyl group positioned near an enzyme residue that will act as a general base, B_2. The general base abstracts a proton from the methyl group of AcCoA which will generate the enol (or enolate), stabilized as suggested above, and this step likely comes to equilibrium prior to formation of homocitryl-CoA. A nucleophilic attack of the methyl of AcCoA on the carbonyl of α-Kg is then carried out, giving the alkoxide of homocitryl-CoA, which then accepts a proton from B_1H. The resulting homocitryl-CoA is then hydrolyzed with attack by the Zn-OH to give a tetrahedral intermediate that collapses, likely aided by B_1 acting as a general base. The resulting carboxylate may still be coordinated to Zn prior to release of homocitrate.

ACKNOWLEDGMENT

We thank Dr. Babak Andi and Dr. William E. Karsten for insightful discussion of the results and technical assistance on experimental protocol and data analysis.

REFERENCES

1. Tucci, A. F., and Ceci, L. N. (1972) Homocitrate synthase from yeast, *Arch. Biochem. Biophys. 153*, 742−750.
2. Gray, G. S., and Bhattacharjee, J. K. (1976) Biosynthesis of lysine in *Saccharomyces cerevisiae*: properties and spectrophotometric determination of homocitrate synthase activity, *Can. J. Microbiol. 22*, 1664−1667.
3. Xu, H., Andi, B., Qian, J., West, A. H., and Cook, P. F. (2006) The α-aminoadipate pathway for lysine biosynthesis in fungi, *Cell Biochem. Biophys. 46*, 43−64.
4. Johansson, E., Steffens, J. J., Lindqvist, Y., and Schneider, G. (2000) Crystal structure of saccharopine reductase from *Magnaporthe grisea*, an enzyme of the α-aminoadipate pathway of lysine biosynthesis, *Structure 8*, 1037−1047.
5. Zheng, L. M., White, R. H., and Dean, D. R. (1997) Purification of the *Azotobacter vinelandii nifV*-encoded homocitrate synthase, *J. Bacteriol. 179*, 5963−5966.
6. Gaillardin, C. M., Poirier, L., and Heslot, H. (1976) A kinetic study of homocitrate synthase activity in the yeast *Saccharomycopsis lipolytica*, *Biochim. Biophys. Acta 422*, 390−406.
7. Jaklitsch, W. M., and Kubicek, C. P. (1990) Homocitrate synthase from *Penicillium chrysogenum*, *Biochem. J. 269*, 247−253.
8. Andi, B., West, A. H., and Cook, P. F. (2004) Stabilization and characterization of histidine-tagged homocitrate synthase from *Saccharomyces cerevisiae*, *Arch. Biochem. Biophys. 421*, 243−254.
9. Andi, B., West, A. H., and Cook, P. F. (2004) Kinetic mechanism of histidine-tagged homocitrate synthase from *Saccharomyces cerevisiae*, *Biochemistry 43*, 11790−11795.
10. Bunik, V. I., Denton, T. T., Xu, H., Thompson, C. M., Cooper, A. J. L., and Gibson, G. E. (2005) Phosphonate analogues of α-ketoglutarate inhibit the activity of the α-ketoglutarate dehydrogenase complex isolated from brain and in cultured cells, *Biochemistry 44*, 10552−10561.
11. Simon, E. J., and Shemin, D. (1953) The preparation of *S*-succinyl coenzyme A, *J. Am. Chem. Soc. 75*, 2520.
12. Padmakumar, R., Padmakumar, R., and Banerjee, R. (1997) Large-scale synthesis of coenzyme A esters, *Methods Enzymol. 279*, 220−225.
13. Kosicki, G. W., and Srere, P. A. (1961) Deuterium isotope rate effects with citrate-condensing enzyme, *J. Biol. Chem. 236*, 2566−2570.
14. Roeder, P. R., and Kohlhaw, G. B. (1980) Alpha-isopropylmalate synthase from yeast a zinc metalloenzyme, *Biochim. Biophys. Acta 613*, 482−487.
15. Koon, N., Squire, C. J., and Baker, E. N. (2004) Crystal structure of LeuA from *Mycobacterium tuberculosis*, a key enzyme in leucine biosynthesis, *Proc. Natl. Acad. Sci. U.S.A. 101*, 8295−8300.
16. Vallee, B. L., and Auld, D. S. (1990) Active-site zinc ligands and activated H_2O of zinc enzymes, *Proc. Natl. Acad. Sci. U.S.A. 87*, 220−224.
17. Vallee, B., and Auld, D. S. (1989) Short and long spacer sequences and other structural features of zinc binding sites in zinc enzymes, *FEBS Lett. 257*, 138−140.
18. Vallee, B., and Auld, D. S. (1990) Zinc coordination, function, and structure of zinc enzymes and others proteins, *Biochemistry 29*, 5647−5659.
19. Majamaa, K., Hanauske-abel, H. M., Günzler, V., and Kivirikko, K. I. (1984) The 2-oxoglutarate binding site of proyl 4-hydroxylase: identification of distinct subsites and evidence for 2-oxoglutarte decarboxylation in a ligand reaction at the enzyme-bound ferrous ion, *Eur. J. Biochem. 138*, 239−245.
20. Majamaa, K., Turpeenniemi-hujanen, T. M., Latipää, P., Günzler, V., Hanauske-Abel, H. M., Hassinen, I. E., and Kivirikko, K. I. (1985) Differences between collagen hydroxylases and 2-oxoglutarate dehydrogenase in their inhibition by structural analogues of 2-oxoglutarate, *Biochem. J. 229*, 127−133.
21. Ng, S.-F., Hannauske-Abel, H. M., and Englard, S. (1991) Cosubstrate binding site of *Pseudomonas* sp. AK1 γ-butyrobetaine hydroxylase: interactions with structural analogs of α-ketogluatrate, *J. Biol. Chem. 266*, 1526−1533.
22. Cleland, W. W. (1977) Determination the chemical mechanisms of enzyme-catalyzed reactions by kinetic studies, *Adv. Enzymol. Relat. Areas Mol. Biol. 45*, 273−387.
23. Johnson, C., Roderick, S. L., and Cook, P. F. (2005) The serine acetyltransferase reaction: acetyl transfer from an acylpantothenyl donor to an alcohol, *Arch. Biochem. Biophys. 433*, 85−95.
24. Dawson, R. M. C., Elliott, D. C., Elliott, W. H., and Jones, K. M. (1991) *Data for Biochemical Research*, 3rd ed., p 118, Oxford University Press, New York.
25. Andi, B., West, A. H., and Cook, P. F. (2005) Regulatory mechanism of histidine-tagged homocitrate synthase from *Saccharomyces cerevisiae*: I. Kinetic studies, *J. Biol. Chem. 280*, 31624−31632.
26. Andi, B., and Cook, P. F. (2005) Regulatory mechanism of histidine-tagged homocitrate synthase form *Saccharomyces cerevisae*: II. Theory, *J. Biol. Chem. 280*, 31633−31640.

27. Cleland, W. W. (1980) Measurement of isotope effects by the equilibrium perturbation technique, *Methods Enzymol. 64*, 104−125.
28. Rendina, A. R., Hermes, J. D., and Cleland, W. W. (1984) A novel method for determining rate constants for dehydration of aldehyde hydrates, *Biochemistry 23*, 5148−5156.
29. Gruen, L. C., and McTigue, P. T. (1963) Hydration equilibria of aliphatic aldehydes in H_2O and D_2O, *J. Chem. Soc. 166*, 5217−5223.

BI060889H